JACC: CARDIOVASCULAR IMAGING VOL. 5, NO. 12, 2012

ISSN 1936-878X/$36.00
PUBLISHED BY ELSEVIER INC. http://dx.doi.org/10.1016/j.jcmg.2012.03.019

The Napkin-Ring Sign Indicates Advanced Atherosclerotic Lesions in Coronary CT Angiography

Pál Maurovich-Horvat, MD, PhD,*† Christopher L. Schlett, MD, MPH,* Hatem Alkadhi, MD, MPH,* Masataka Nakano, MD,‡ Fumiyuki Otsuka, MD,‡ Paul Stolzmann, MD,* Hans Scheffel, MD,* Maros Ferencik, MD, PhD,* Matthias F. Kriegel, MD,* Harald Seifarth, MD,* Renu Virmani, MD,‡ Udo Hoffmann, MD, MPH*

Boston, Massachusetts; Gaithersburg, Maryland; and Budapest, Hungary

OBJECTIVES This study sought to determine the accuracy of plaque pattern assessment by coronary computed tomography angiography (CCTA) to differentiate between early and advanced atherosclerotic lesions as defined by histology.

BACKGROUND A ringlike attenuation pattern of coronary atherosclerotic plaques termed as napkin-ring sign (NRS) was described in CCTA of patients who had acute coronary syndrome.

METHODS All procedures were performed in accordance with local and federal regulations and the Declaration of Helsinki. Approval of the local ethics committees was obtained. We investigated 21 coronary arteries of 7 donor hearts. Overall, 611 histological sections were obtained and coregistered with CCTA images. The CCTA cross sections were read in random order for conventional plaque categories (noncalcified [NCP], mixed [MP], calcified [CP]) and plaque patterns (homogenous, heterogeneous with no napkin-ring sign [non-NRS], and heterogeneous with NRS).

RESULTS No plaque was detected in 134 (21.9%), NCP in 254 (41.6%), MP in 191 (31.3%), and CP in 32 (5.2%) CCTA cross sections. The NCP and MP were further classified into homogenous plaques (n = 207, 46.5%), non-NRS plaques (n = 200, 44.9%), and NRS plaques (n = 38, 8.6%). The specificities of NCP and MP to identify advanced lesions were moderate (57.9%, 95% confidence interval [CI]: 50.1% to 65.6%, and 72.1%, 95% CI: 64.7% to 79.4%, respectively), which were similar to the homogenous and heterogeneous plaques (62.6%, 95% CI: 54.8% to 70.3%, and 67.3%, 95% CI: 58.6% to 76.1%, respectively). In contrast, the specificity of the NRS to identify advanced lesions was excellent (98.9%, 95% CI: 97.6% to 100%). The diagnostic performance of the pattern-based scheme to identify advanced lesions was significantly better than that of the conventional plaque scheme (area under the curve: 0.761 vs. 0.678, respectively; p = 0.001).

CONCLUSIONS The assessment of the plaque pattern improves diagnostic accuracy of CCTA to identify advanced atherosclerotic lesions. The CCTA finding of NRS has a high specificity and high positive predictive value for the presence of advanced lesions. (J Am Coll Cardiol Img 2012;5:1243–52)

From the *Cardiac MR PET CT Program, Department of Radiology, Massachusetts General Hospital and Harvard Medical School, Boston, Massachusetts; †Heart Center, Semmelweis University, Budapest, Hungary; and the ‡CV Path Institute Inc., Gaithersburg, Maryland. This work was supported by an unrestricted grant from GE Healthcare. Dr. Maurovich-Horvat received support from grant no. TÁMOP-4.2.1/B-09/1/KMR-2010-0001. Dr. Seifarth was supported by a grant from Deutsche Forschungsgemeinschaft (grant no. DFG Se 2029/1-1). Dr. Virmani has been a consultant to Terumo Corporation, from whom he has received research grant support. All other authors have reported that they have no relationships relevant to the contents of this paper to disclose.

Manuscript received September 12, 2011; revised manuscript received February 8, 2012, accepted March 2, 2012.

Atherosclerotic plaque rupture and subsequent coronary artery thrombosis is the most common cause of sudden coronary deaths (1). Rupture-prone plaques are advanced atherosclerotic lesions characterized by a large necrotic core and a markedly attenuated fibrotic cap. This type of plaque is often referred to as vulnerable plaque (2,3). Recently, coronary computed tomography angiography (CCTA) has become a clinically established tool for the diagnosis of significant coronary artery disease (4–6). In addition, CCTA permits the assessment of coronary atherosclerotic plaque morphology and composition in good agreement with intravascular ultrasound (6,7). Given the complex morphology and composition of the advanced plaques, the current classification into noncalcified plaque (NCP), calcified plaque (CP), and mixed plaque (MP) is crude and provides only limited information regarding the risk of individual plaques to cause clinical events (2,8). To address this issue (1,9–11), several investigators have recently attempted a more differentiated assessment of NCP and described a ringlike attenuation of the noncalcified portion of the coronary atherosclerotic lesion, which was termed napkin-ring sign (NRS). This sign has been associated with high-risk plaques in several studies (12–17).

ABBREVIATIONS AND ACRONYMS

AIT = adaptive intimal thickening
AUC = area under the curve
CCTA = coronary computed tomography angiography
CI = confidence interval(s)
CP = calcified plaque
CT = computed tomography
EFA = early fibroatheroma
Fib = fibrous plaque
HU = Hounsfield unit(s)
LFA = late fibroatheroma
MP = mixed plaque
NCP = non-calcified plaque
NRS = napkin-ring sign
PAP = plaque attenuation pattern
PIT = pathological intimal thickening
TCFA = thin cap fibroatheroma

In this study, we sought to determine the reliability to qualitatively assess and differentiate attenuation patterns of NCP by CCTA under ex vivo conditions. Furthermore, we sought to determine the diagnostic performance of a plaque attenuation pattern (PAP)-based classification scheme to differentiate between early and advanced atherosclerotic plaques as defined by histopathology. Moreover, we sought to assess whether this new classification provides incremental value to the currently used classification of atherosclerotic lesions by CCTA.

METHODS

All procedures were approved by the institutional ethics committees and were performed in accordance with local and federal regulations and the Declaration of Helsinki. The donor hearts were provided by the International Institute for the Advancement of Medicine (Jessup, Pennsylvania). The inclusion criteria were the following: donor age between 40 and 70 years, male sex, and history of myocardial infarction or coronary artery disease proven by diagnostic tests. Donors who underwent coronary artery bypass graft surgery were excluded from this study. The maximum allowed warm ischemia time was 6 h, and the maximum allowed cold ischemia time was 15 h. Seven isolated donor hearts (the median age of the donors: 53 years, range 42 to 61 years) were investigated. The cause of death was stroke in 6 cases, and in 1 case, the cause of death was non-natural (suicide).

Heart preparation and CCTA imaging. To prepare donor hearts, the right and the left coronary arteries were selectively cannulated and the coronaries were flushed with saline to remove air bubbles and superficial thrombi. A rubber balloon filled with 50 to 100 ml water was placed in the left ventricle to retain the physiological shape of the heart. The organ was positioned in the center of a canola oil tank to simulate the pericardial adipose tissue layer. The oil tank was secured on the CT table and an in-house prepared contrast agent was injected in the coronary arteries. To achieve an intraluminal contrast enhancement similar to in vivo CCTA, methylcellulose (Methocel, DOW Chemical Company, Midland, Michigan) with 3% iopamidol contrast agent (Isovue 370, Bracco Diagnostics, Milan, Italy) was used. All CT data acquisition was performed with a 64-detector row CT scanner (High-Definition, GE Discovery, CT 750HD, GE Healthcare, Milwaukee, Wisconsin) using a sequential acquisition mode. The scan parameters were the following: 64 × 0.625 mm collimation; 0.35-s rotation time; tube voltage of 120 kV; tube current time product of 500 mAs. The entire dataset was reconstructed using an adaptive statistical iterative reconstruction technique (ASIR, GE Healthcare,) with a 40% blend with filtered back-projection. All reconstructed CCTA images were sent to an offline workstation for further analysis (Leonardo, Siemens Healthcare, Erlangen, Germany). Subsequent to the CCTA imaging, the coronary arteries were excised with surrounding tissue and the side branches were ligated. The coronaries were pressure-perfused (130 mm Hg) with 10% buffered neutral formalin solution to achieve tissue fixation. The preparation and the CCTA imaging were completed within 4 h after receiving the heart to avoid potential post-mortem changes of the tissue.

Histology. The histological preparation and analysis was performed by experts specialized in cardiovascular pathology. Paraffin sections were obtained in

1.5-mm and in 2-mm increments (382 cuts and 185 cuts, respectively). Coronary artery segments with minimal atherosclerotic disease were sectioned every 5 mm (44 slides). The thickness of a single histological section was 6 μm. All sections were stained with Movat pentachrome. Each cross section was classified according the modified American Heart Association scheme into the following categories: adaptive intimal thickening (AIT); pathological intimal thickening (PIT); fibrous plaque (Fib); early fibroatheroma (EFA); late fibroatheroma (LFA); thin cap fibroatheroma (TCFA) (18,19). According to a report on atherosclerotic lesion classification from the American Heart Association, the AIT, Fib, and PIT were considered early atherosclerotic lesions, and EFA, LFA, and TCFA were categorized as advanced lesions (20). The differentiation between early and advanced atherosclerotic lesions is based on histological criteria, where the terms mean both time-dependent development and complexity of atheroma formation (20). Advanced lesions are associated with vulnerability and with a higher risk of a subsequent clinical event (2,18,20,21).

In addition to the analysis of the individual cross sections, we stratified each of the 21 vessels into individual atherosclerotic plaques. A plaque was defined as at least 1 cross section with Fib, EFA, LFA, or TCFA and separated (from the next lesion) by at least 1 cross section with AIT or PIT. A plaque was defined as advanced atherosclerotic plaque if it contained at least 1 cross section with EFA, LFA, or TCFA.

Coregistration of histology and CCTA. An experienced investigator, who did not take part in the image assessment, performed the coregistration of CCTA and histology images. A multiplanar reconstruction technique was used to generate CCTA images perpendicular to the vessel centerline at the position of the histological cuts. A combined mathematical and anatomical approach was used to match the CCTA and histological images. As the first step, we calculated the distance of each image cross section from the 0-reference point (distal end of the plastic luer). Second, we used anatomical markers visible on both CCTA and histology, such as side branches, bifurcations, and features of vessel wall morphology (e.g., plaque shape, calcification pattern, orientations of the myocardium and pericardial adipose tissue layer) to match the position and set the rotational orientation of each image.

Plaque classification. An experienced CCTA reader (P. M.-H., who has 6 years of experience) performed the qualitative reading of all CCTA cross sections and assessed the images for the presence and composition of plaque as will be described. A second experienced observer (H. A., who has 8 years of experience) independently performed analyses of 100 randomly selected cross sections to calculate interobserver variability. Initially, plaque was characterized as NCP, CP, or MP (containing both components). Specifically, any discernible structure that could be assigned to the coronary artery wall, but with a CT density below the contrast-enhanced coronary lumen and above the surrounding connective tissue, was defined as noncalcified coronary atherosclerotic plaque (22). Any hyperdense structure that could be visualized separately from the contrast-enhanced coronary lumen (either because it was "embedded" within NCP or because its density was above the contrast-enhanced lumen) and could be assigned to the coronary artery wall was defined as calcified atherosclerotic plaque (22).

A second qualitative reading was performed to describe the attenuation pattern of NCP in cross sections previously classified as NCP or MP. A plaque cross section was classified as heterogeneous if at least 2 regions of different attenuation could be visually distinguished within the noncalcified portion, whereas the plaque was classified as homogenous if no such distinction could be made. Plaque cross sections with a heterogeneous attenuation pattern were further subclassified into plaques with and without NRS (15). NRS was defined as the presence of low CT attenuation in the center of the plaque close to the lumen surrounded by a rim area of higher attenuation (15). Heterogeneous plaques were identified as non-NRS plaques if the pattern of low and high attenuation was spatially nonstructured or random. Thus, the PAP classification scheme comprised 3 categories: homogenous plaque; non-NRS heterogeneous plaque; and NRS heterogeneous plaque (Fig. 1). All readings were performed with a fixed window setting (700 Hounsfield units [HU] width, 200 HU level).

Statistical analysis. Continuous variables were expressed as mean ± SD, and categorical variables were expressed as frequencies or percentages. To determine interobserver variability, an independent reader assessed a random subset of 100 cross-registered CCTA images for conventional plaque categories and PAP. The interobserver agreement was evaluated using Cohen kappa statistics that were interpreted as follows. A k value greater than

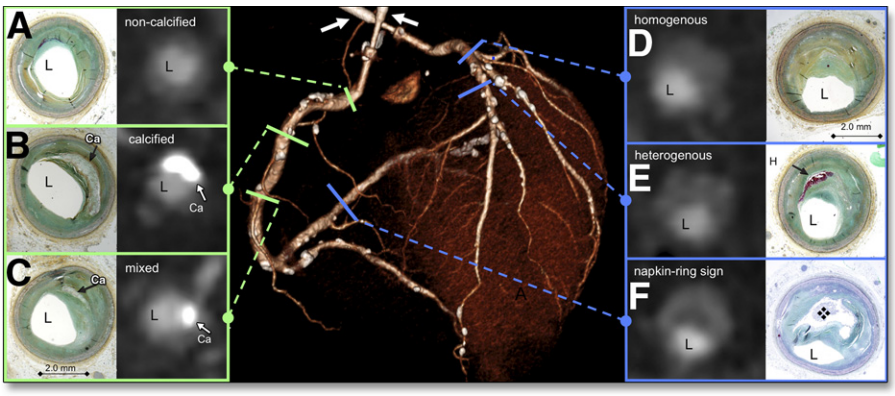

Figure 1. Traditional and PAP-Based Plaque Classifications as Assessed by CT

The **center** illustrates a volume-rendered coronary computed tomography angiography (CCTA) of an ex vivo donor heart with the anatomical position of the plaque cross sections. The **white arrows** indicate the plastic luers and canules that were used to fill the coronaries with the methylcellulose-based iodinated contrast mixture. The traditional plaque classification comprises noncalcified **(A),** calcified **(B),** and mixed **(C)** plaques. Whereas the plaque attenuation pattern (PAP)-based scheme includes homogeneous **(D),** heterogeneous **(E),** and NRS **(F)** plaques. The corresponding histology slides: pathological intimal thickening **(A);** fibrous plaque with sheet calcification **(B);** pathological intimal thickening with spotty calcification **(C);** fibrous plaque **(D);** early fibroatheroma with intraplaque hemorrhage **(E),** and late fibroatheroma with large necrotic core **(F).** Ca = calcification; H = hemorrhage; L = lumen; diamond sign = necrotic core.

0.80 corresponded to an excellent agreement, and a kappa value of 0.61 to 0.80 corresponded to a good interobserver agreement (23).

For all remaining analysis, cross sections containing purely calcified plaque on CCTA were excluded.

We determined whether the distribution of the PAP categories (homogenous, heterogeneous with and without the NRS) differed between traditional plaque categories (NCP, MP) and whether the frequency of advanced lesions (defined as EFA, LFA, or TCFA) and TFCA differed significantly within PAP categories (homogenous, heterogeneous with and without the NRS) and traditional plaque categories (NCP, MP). To test for statistical significance, Fisher exact test was used for 2 × 2 tables and chi-squared test for tables with more rows or columns.

To determine the diagnostic accuracy of CT-based plaque composition (both conventional and attenuation pattern–based classification) for the detection of advanced lesions and TFCA sensitivity, specificity, negative predictive value, and positive predictive value were calculated from 2 × 2 contingency tables. We calculated binomial 95% confidence intervals (CI), as well 95% CI adjusted for the correlated data structure on a per lesion level. For this, a SAS (SAS Institute Inc., Cary, North Carolina) macro has been written using a within-cluster correlation estimator (24,25). Adjusted 95% CI have been reported if not otherwise specified.

To assess further the diagnostic capacity CCTA to detect advanced lesions and TFCA, the C-statistic was used. In the first step, the categories for each classification scheme were sorted separately by their likelihood ratio for advanced lesions and TFCA. Next, separated logistic regression models for each scheme were fitted, and C-statistics were derived, which are equivalent to the area under the receiver-operating characteristics curve (AUC) (26). The asymptotic 95% CI for the AUC were estimated using a nonparametric approach, which is closely related to the jackknife technique as proposed by DeLong et al. (27) and comparisons in AUC/C-statistics were performed by using a contrast matrix. All statistical tests were performed by using software SAS (version 9.2). A p value of <0.05 was considered statistically significant.

RESULTS

Overall, 611 histological sections from 21 coronary arteries of 7 donor hearts were investigated. The average studied vessel length was 67 mm (range 25 to 110 mm). Of the 611 sections, 71 (11.6%) were identified as AIT, 222 (36.3%) as PIT, 179 (29.3%) as Fib, 59 (9.7%) as EFA, 60 (9.8%) as LFA, and 20 (3.3%) contained TCFA. The proportion of early lesions (AIT, PIT, Fib) versus advanced lesions (EFA, LFA, TCFA) was 77.3% (n = 472) versus 22.7% (n = 132). All matched CCTA cross

Table 1. Comparison of PAP Categories to the Conventional CT Plaque Classification Scheme

		Heterogeneous			
	Homogenous	All	Non-NRS	NRS	Total
Noncalcified plaque	130 (62.8)	124 (52.1)	105 (52.5)	19 (50)	254 (57.1)
Mixed plaques	77 (37.2)	114 (47.9)	95 (47.5)	19 (50)	191 (42.9)
Total	207	238	200	38	445

Values are n (%) or n.
CT = computed tomography; NRS = napkin-ring sign; PAP = plaque attenuation pattern.

sections (n = 611) were eligible for comparison with histology.

Plaque classification. Among the 611 coregistered CT cross sections, no plaque was detected in 134 (21.9%), NCP in 254 (41.6%), MP in 191 (31.3%), and CP in 32 (5.2%) cross sections. Among the 445 cross sections containing NCP or MP, a homogenous pattern of plaque attenuation was found in 207 (46.5%) cross sections (130 for NCP and 77 for MP; 62.8% vs. 37.2%, respectively) and a heterogeneous pattern was found in 238 (53.5%) cross sections (124 for NCP and 114 for MP; 52.1% vs. 47.9%, respectively) (Table 1, Fig. 2). Thus, homogenous plaques were somewhat less frequently found among MP than among NCP (p = 0.03).

Heterogeneous plaques were further classified as non-NRS or NRS plaques (Table 1, Fig. 2). Among the 238 cross sections with a heterogeneous pattern, non-NRS lesions were identified in 200 (84.0%) cross sections (105 with NCP and 95 with MP; 52.5% vs. 47.5%, respectively) and NRS was identified in 38 (16.0%) cross sections (19 in NCP and 19 in MP, 50% vs. 50%, respectively). Thus, there was no significant difference regarding the distribution of NRS or non-NRS plaques across NCP and MP plaques (p = 0.86), suggesting that the presence of NRS was independent of the conventional categories of NCP or MP.

Interobserver variability. In the subgroup of 100 cross sections, the interobserver agreement between the 2 CT readers to classify CCTA cross sections as no plaque, NCP, MP, or CP was excellent (Cohen kappa = 0.83; 95% CI: 0.73 to 0.94) with the majority of the disagreements occurring between a normal vessel wall and the presence of NCP. The interobserver agreement between the 2 CT readers to classify plaques as no plaque, homogenous plaque, non-NRS heterogeneous plaque, NRS, or NRS plaque) was good (Cohen kappa = 0.61; 95% CI: 0.56 to 0.67) with the majority of disagreements occurring between a normal vessel wall and the presence of a heterogeneous or homogenous NCP. In contrast, the interobserver variability to detect NRS was excellent (Cohen kappa = 0.86; 95% CI: 0.76 to 0.96).

Association of CCTA plaque type with histopathology. Overall, 99.3% (n = 133) of CT cross sections without plaque were early lesions according to histology. There was no association between the conventional classification of NCP and MP and early and advanced atherosclerotic lesions as classified by histology (advanced lesions; NCP: 50.8% [n = 68] vs. MP: 49.2% [n = 66]; p = 0.06) (Table 2).

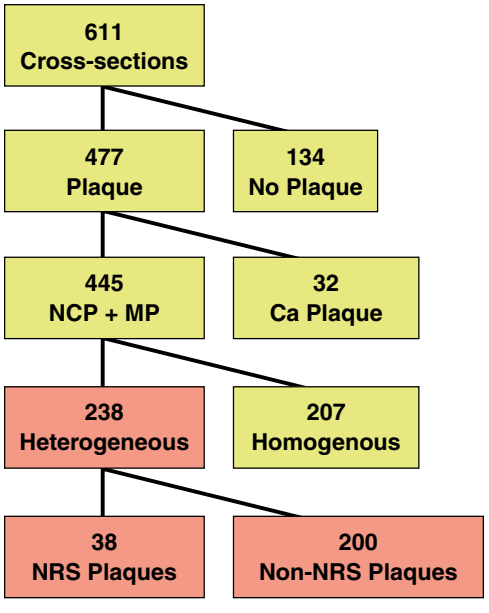

Figure 2. Classification of Plaques According to the PAP Scheme

Among the 611 coregistered computed tomography cross sections, no plaque was detected in 134, noncalcified plaque (NCP) or mixed plaque (MP) in 445, and calcified (Ca) plaque in 32 cross sections. Among the cross sections containing NCP or MP, a homogenous plaque pattern was found in 207 cross sections and a heterogeneous pattern was found in 238 cross sections. Among the 238 cross sections with a heterogeneous pattern, napkin-ring sign (NRS) lesions were identified in 38 cross sections and non-NRS lesions in 200 cross sections. PAP = plaque attenuation pattern.

Table 2. Comparison of Conventional Plaque Classification and Intra-PAP–Based Classification Schemes With Histopathology

	Early	Advanced	Total	p Value
No plaque	133 (30)	1 (0.7)	134 (23.1)	
Conventional scheme				0.06
Noncalcified	187 (41.9)	67 (50.4)	254 (43.9)	
Mixed	124 (28.1)	67 (48.9)	191 (33.0)	
PAP scheme				<0.0001
Homogenous	166 (37.4)	41 (30.4)	207 (35.8)	
Heterogeneous non-NRS	140 (31.5)	60 (44.5)	200 (34.5)	
Heterogeneous NRS	5 (1.1)	33 (24.4)	38 (6.6)	

Values are n (%).
Abbreviations as in Table 1.

In contrast, differences in the distribution of early and advanced atherosclerotic lesions were found when the plaques were classified as heterogeneous and homogenous according to CCTA. Overall, 69.4% (93 of 134) of advanced lesions were classified as heterogeneous plaque on CCTA and only 30.6% (41 of 134) as homogenous plaque ($p < 0.0001$) (Table 2). Among the 38 heterogeneous plaques classified as NRS, the majority (86.8% [33 of 38]) were classified as advanced atherosclerotic lesions by histopathology ($p < 0.0001$) (Fig. 3).

In general, these associations were similar for the subgroup of 20 plaques (3.3%) characterized as TCFA in histopathology. There were no TCFA present in normal CCTA cross sections, and there was no association between the distribution of TCFA in plaques classified as NCP or MP ($p = 0.63$). In contrast, the frequency of TCFA differed across plaques characterized as heterogeneous or homogenous by CCTA with the majority (83.3%) of TCFA being classified as heterogeneous plaques ($p = 0.01$). Among the 15 TCFA lesions described as heterogeneous in CCTA, 5 (33.3%) demonstrated NRS ($p = 0.07$).

Diagnostic accuracy. Table 3 presents the diagnostic accuracy measures of conventional and pattern-based CCTA plaque categories to identify advanced atherosclerotic lesions. The heterogeneous plaque category, showed a good sensitivity, specificity, and negative predictive value to identify advanced lesions (68.9%, 67.3%, and 87.7%, respectively). The NRS category showed the highest specificity value among all CCTA plaque categories for the presence of advanced lesions and TFCA in histopathology (98.9%, 95% CI: 97.6% to 100%, and 94.1%, 95% CI: 90.8% to 97.4%, respectively) (Table 3).

Diagnostic accuracy was on average 61% for the conventional plaque categories (56.0% for NCP and 66.8% MP), and it ranged from 55% to 82% for the pattern-based analysis (55.1% for homogenous,

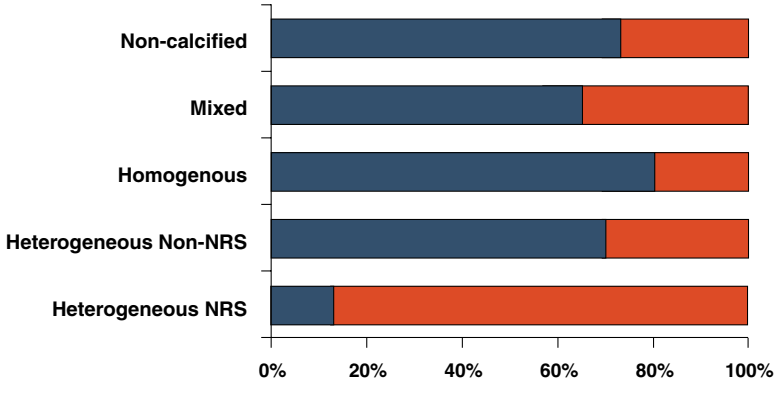

Figure 3. Percentage of Early and Advanced Atherosclerotic Lesions Among the Traditional and Plaque Attenuation–Based CT Plaque Types

The **blue bars** represent early atherosclerotic lesions, whereas the **red bars** represent advanced atherosclerotic lesions. The percentage of advanced atherosclerotic lesions among different CT plaque types: noncalcified plaques: 26.4% (67 of 254); mixed plaques: 35.1% (67 of 191); homogenous plaques: 19.8% (41 of 207); non-NRS plaques: 30.0% (60 of 200); NRS plaques: 86.8% (33 of 38). Abbreviations as in Figures 1 and 2.

Table 3. Diagnostic Accuracy of Different Qualitative Plaque Categories for CCTA to Identify Advanced Lesions as Classified by Histology With 95% CI

	Sensitivity % ($n_{TruePos}/n_{DiseasePos}$)	Specificity % ($n_{TrueNeg}/n_{DiseaseNeg}$)	PPV % ($n_{TruePos}/n_{TestPos}$)	NPV % ($n_{TrueNeg}/n_{TestNeg}$)
Any plaque	99.3 (134/135)	30.0 (133/444)	30.1 (134/445)	99.3 (133/134)
Crude 95% CI	95.9–99.9	25.7–34.5	25.9–34.6	95.9–100
Adjusted 95% CI	97.6–100	20.5–39.4	23.1–37.1	94.8–100
PAP classification				
Homogenous	30.4 (41/135)	62.6 (278/444)	19.8 (41/207)	74.7 (278/372)
Crude 95% CI	22.8–38.9	57.9–67.1	14.6–25.9	70.0–79.1
Adjusted 95% CI	14.8–45.9	54.8–70.3	11.0–28.6	65.7–83.8
Heterogeneous	68.9 (93/135)	67.3 (299/444)	39.1 (93/238)	87.7 (299/341)
Crude 95% CI	60.4–76.6	52.8–71.7	32.8–45.6	83.7–90.1
Adjusted 95% CI	53.0–84.8	58.6–76.1	27.3–50.8	82.0–93.3
Non-NRS plaque	44.4 (60/135)	68.5 (304/444)	30.0 (60/200)	80.2 (304/379)
Crude 95% CI	35.9–53.2	63.9–72.8	23.7–36.9	75.8–84.1
Adjusted 95% CI	31.6–57.3	60.2–76.7	18.7–41.3	72.8–87.6
NRS plaque	24.4 (33/135)	98.9 (439/444)	86.8 (33/38)	81.2 (439/541)
Crude 95% CI	17.5–32.6	97.4–99.6	71.9–95.6	77.6–84.4
Adjusted 95% CI	12.1–36.8	97.6–100	62.7–100	76.1–86.2
Conventional plaque classification				
Noncalcified plaque	49.6 (67/135)	57.9 (257/444)	26.4 (67/254)	79.1 (257/325)
Crude 95% CI	40.9–58.3	53.1–62.5	21.1–32.3	74.2–83.4
Adjusted 95% CI	31.0–68.3	50.1–65.6	17.7–35.1	71.0–87.2
Mixed plaque	49.6 (67/135)	72.1 (320/444)	35.1 (67/191)	82.5 (320/388)
Crude 95% CI	40.9–58.4	67.7–76.2	28.3–42.3	78.3–86.1
Adjusted 95% CI	30.8–68.4	64.7–79.4	22.9–47.2	75.5–89.5

Confidence intervals are provided for a crude binomial analysis and adjusted for the within-lesion correlation.
CCTA = coronary computed tomography; CI = confidence interval; DiseaseNeg = disease negative; DiseasePos = disease positive; NPV = negative predictive value; PPV = positive predictive value; TestPos = test positive cross section; TestNeg = test negative cross section; TrueNeg = true negative cross sections; TruePos = true positive cross sections; other abbreviations as in Tables 1 and 2.

67.7% for heterogeneous, and 81.5% for NRS plaques). Comparing the diagnostic performance of the 2 different schemes, the plaque classification scheme based on attenuation pattern had a significantly better discriminative power than did the conventional scheme to identify both advanced lesions as well TCFA as defined by histopathology (AUC: 0.761 vs. 0.678, p = 0.001, and 0.769 vs. 0.648, p = 0.02, respectively) (Fig. 4).

Per-lesion analysis. In addition, we have performed a per plaque analysis. We have identified 95 individual plaques based on histological criteria. Out of this highly diseased sample, 50 plaques were classified as advanced lesions as they contained at least 1 cross section with EFA, LFA, or TCFA; 45 plaques were classified as early lesion because they contained only AIT, PIT, or Fib. Blinded to the histology results, CT readers identified NRS in 38 of 611 cross sections, 18 of 95 individual plaques, and 6 of 7 donor hearts. Notably, all of the individual plaques containing NRS were advanced lesions according to the histology. A per-plaque analysis led to specificity of 100% (95% CI: 92.0% to 100%) and a sensitivity of 36.0% (95% CI: 22.9% to 50.8%) for NRS to identify advanced lesion.

DISCUSSION

The current clinically used CCTA classification of coronary atherosclerotic plaque composition is based on the presence or absence of calcification and was initially suggested in early CCTA studies using 4-slice multidetector CT technology with limited spatial and temporal resolution (7,22,28–31). Although this classification has demonstrated that presence of NCP has some incremental value over the detection of CP in predicting adverse cardiovascular events (32–36), its ability to distinguish individual plaques that may be at higher risk for cardiovascular events is limited (6,7,37,38). Our data demonstrates that a qualitative assessment of the attenuation pattern of NCP by CCTA under ex vivo conditions significantly improves diagnostic accuracy for the detection of advanced plaque and TCFA as determined by histopathology compared with the conventional assessment of plaque composition ($p < 0.05$ for both). Remark-

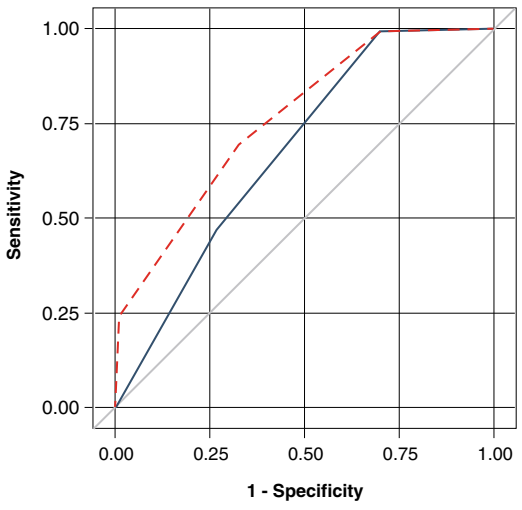

Figure 4. ROC Curves to Compare AUC of PAP Scheme Versus Conventional Scheme

The area under the receiver-operating characteristic curve was 0.678 for conventional plaque classification scheme **(blue line)** and 0.761 for plaque attenuation pattern (PAP) scheme **(red line).** The PAP scheme had a higher diagnostic performance than the conventional plaque scheme does, p = 0.001. AUC = area under the curve; ROC = receiver-operating characteristic.

ably, both heterogeneous appearances of NCP and NRS are highly specific for the presence of both advanced plaque and TFCA in histopathology (specificity: 98.9% and 94.1%, respectively).

Previous studies demonstrated the inability of density measurements within the plaque to differentiate reliably between lipid-rich and fibrous plaques because of a significant overlap in attenuation values (30,39–41). Significant progress in CT technology with an improvement of spatial resolution reaching 0.3 mm in-plane, allows a more differentiated assessment of the noncalcified portion of plaque. Recent studies suggest that low attenuation (<30 HU) is a hallmark of both culprit lesions in acute coronary syndromes and is more frequently found in plaques that are at high risk for rupture (12–15). In addition, higher spatial resolution may mitigate the "masking" of NCP by CP, which appears at least 4× larger in CT than its actual size due to blooming artifacts (42).

Our results demonstrate the increased ability of CCTA to differentiate individual plaque characteristics that are specific for advanced atherosclerotic lesions associated with increased vulnerability and subsequent adverse cardiovascular events (2,18,20,21).

Whereas the current clinically used classifications of MP and NCP are unable to predict the presence of advanced plaques, NRS demonstrated a 98.9% specificity to identify advanced lesions and a 92.3% specificity for identifying TCFA. Our finding that the frequency of NRS was similar in MP and in NCP may help to resolve some contradictions in published studies, some of them reporting that MP rather than NCP indicates a higher risk for future cardiovascular events (29,32–36,43,44). Our data suggest that certain qualities of NCP irrespective of the presence of calcium are associated with advanced atherosclerotic lesions. Prospective clinical studies are warranted to determine the prognostic value of PAP assessment to identify patients with the highest risk of developing cardiovascular events (9).

The current study further demonstrates that the absence of plaque in CCTA basically excludes the presence of advanced atherosclerotic lesion or TFCA. This finding is consistent with clinical studies demonstrating the rarity of cardiovascular events in patients without coronary artery disease as described by CCTA (29,32–34,43,44).

Whereas quantitative analysis of NCP has been described before, we pursued a qualitative approach to plaque characterization based on initial encouraging findings (15). The qualitative plaque pattern assessment may be more feasible and easier to implement in clinical practice or large studies. In addition, the quantitative assessment of plaque attenuation might be significantly altered by the coronary lumen enhancement, the reconstruction kernel, and the size and number of regions of interest used for the attenuation assessment (40,45).

The ex vivo CCTA imaging was performed in an ideal, motion-free experimental setting. This might limit the direct translation of our findings into in vivo circumstances. Furthermore, our observations are based on only 7 hearts, thus the generalizability of the results might be limited. However, it is important to note that some recently published studies observed a ringlike attenuation pattern similar to that of NRS in patients presenting with acute coronary syndromes (12–14,17). These observations indicate that the qualitative PAP assessment might be feasible in clinical scenarios. Further improvements in acquisition and post-processing techniques (e.g., iterative reconstruction techniques) in combination with reduction in radiation dose may further enhance the ability of CCTA to differentiate between individual plaque components and broaden the applicability of CCTA for the evaluation of coronary atherosclerosis. A sequential imaging strategy using CCTA to identify high-risk plaque features such as the NRS, followed by invasive imaging tools to confirm the presence of

vulnerable plaques might provide a framework suitable to identify individuals with the highest risk to develop acute coronary syndromes. Further ex vivo and in vivo research is warranted to assess the generalizability of our findings.

CONCLUSIONS

The qualitative assessment of the attenuation pattern of NCP tissue improves diagnostic accuracy of CCTA to identify advanced atherosclerotic lesions and TFCA. The CCTA finding of NRS has a high specificity and high positive predictive value for the presence of advanced lesions.

Reprint requests and correspondence: Dr. Udo Hoffmann, Cardiac MR PET CT Program, Massachusetts General Hospital and Harvard Medical School, 165 Cambridge Street Suite 400, Boston, Massachusetts 02114. *E-mail: uhoffmann@partners.org.*

REFERENCES

1. Naghavi M, Libby P, Falk E, et al. From vulnerable plaque to vulnerable patient: a call for new definitions and risk assessment strategies: part I. Circulation 2003;108:1664–72.
2. Virmani R, Burke AP, Farb A, Kolodgie FD. Pathology of the vulnerable plaque. J Am Coll Cardiol 2006;47:C13–8.
3. Virmani R, Burke AP, Kolodgie FD, Farb A. Vulnerable plaque: the pathology of unstable coronary lesions. J Interv Cardiol 2002;15:439–46.
4. Hoffmann U, Ferencik M, Cury RC, Pena AJ. Coronary CT angiography. J Nucl Med 2006;47:797–806.
5. Maurovich-Horvat P, Ghoshhajra B, Ferencik M. Coronary CT angiography for the detection of obstructive coronary artery disease. Curr Cardiovasc Imaging Rep 2010;3:355–65.
6. Achenbach S, Raggi P. Imaging of coronary atherosclerosis by computed tomography. Eur Heart J 2010;31:1442–8.
7. Becker CR, Knez A, Ohnesorge B, Schoepf UJ, Reiser MF. Imaging of noncalcified coronary plaques using helical CT with retrospective ECG gating. AJR Am J Roentgenol 2000;175:423–4.
8. Achenbach S. Can CT detect the vulnerable coronary plaque? Int J Cardiovasc Imaging 2008;24:311–2.
9. Naghavi M, Libby P, Falk E, et al. From vulnerable plaque to vulnerable patient: a call for new definitions and risk assessment strategies: part II. Circulation 2003;108:1772–8.
10. Narula J, Garg P, Achenbach S, Motoyama S, Virmani R, Strauss HW. Arithmetic of vulnerable plaques for noninvasive imaging. Nat Clin Pract Cardiovasc Med 2008;5 Suppl 2:S2–10.
11. Braunwald E. Epilogue: what do clinicians expect from imagers? J Am Coll Cardiol 2006;47:C101–3.
12. Kashiwagi M, Tanaka A, Kitabata H, et al. Feasibility of noninvasive assessment of thin-cap fibroatheroma by multidetector computed tomography. J Am Coll Cardiol Img 2009;2:1412–9.
13. Nakazawa G, Tanabe K, Onuma Y, et al. Efficacy of culprit plaque assessment by 64-slice multidetector computed tomography to predict transient no-reflow phenomenon during percutaneous coronary intervention. Am Heart J 2008;155:1150–7.
14. Tanaka A, Shimada K, Yoshida K, et al. Non-invasive assessment of plaque rupture by 64-slice multidetector computed tomography—comparison with intravascular ultrasound. Circ J 2008;72:1276–81.
15. Maurovich-Horvat P, Hoffmann U, Vorpahl M, Nakano M, Virmani R, Alkadhi H. The napkin-ring sign: CT signature of high risk coronary plaques? J Am Coll Cardiol Img 2010;3:440–4.
16. Donnelly P, Maurovich-Horvat P, Vorpahl M, et al. Multimodality imaging atlas of coronary atherosclerosis. J Am Coll Cardiol Img 2010;3:876–80.
17. Pflederer T, Marwan M, Schepis T, et al. Characterization of culprit lesions in acute coronary syndromes using coronary dual-source CT angiography. Atherosclerosis 2010;211:437–44.
18. Virmani R, Kolodgie FD, Burke AP, Farb A, Schwartz SM. Lessons from sudden coronary death: a comprehensive morphological classification scheme for atherosclerotic lesions. Arterioscler Thromb Vasc Biol 2000;20:1262–75.
19. Kolodgie FD, Gold HK, Burke AP, et al. Intraplaque hemorrhage and progression of coronary atheroma. N Engl J Med 2003;349:2316–25.
20. Stary HC, Chandler AB, Dinsmore RE, et al. A definition of advanced types of atherosclerotic lesions and a histological classification of atherosclerosis: a report from the Committee on Vascular Lesions of the Council on Arteriosclerosis, American Heart Association. Arterioscler Thromb Vasc Biol 1995;15:1512–31.
21. Virmani R, Burke AP, Farb A. Plaque rupture and plaque erosion. Thromb Haemost 1999;82 Suppl 1:1–3.
22. Achenbach S, Moselewski F, Ropers D, et al. Detection of calcified and noncalcified coronary atherosclerotic plaque by contrast-enhanced, submillimeter multidetector spiral computed tomography: a segment-based comparison with intravascular ultrasound. Circulation 2004;109:14–7.
23. Landis JR, Koch GG. The measurement of observer agreement for categorical data. Biometrics 1977;33:159–74.
24. Donner A, Klar N. Confidence interval construction for effect measures arising from cluster randomization trials. J Clin Epidemiol 1993;46:123–31.
25. Genc Y, Gokmen D, Tuccar E, Yagmurlu B. Estimation of sensitivity and specificity for clustered data. Turk J Med Sci 2004;35:21–4.
26. Hanley JA, McNeil BJ. The meaning and use of the area under a receiver operating characteristic (ROC) curve. Radiology 1982;143:29–36.
27. DeLong ER, DeLong DM, Clarke-Pearson DL. Comparing the areas under two or more correlated receiver operating characteristic curves: a nonparametric approach. Biometrics 1988;44:837–45.
28. Becker CR, Ohnesorge BM, Schoepf UJ, Reiser MF. Current development of cardiac imaging with multidetector-row CT. Eur J Radiol 2000;36:97–103.
29. Hoffmann U, Moselewski F, Nieman K, et al. Noninvasive assessment of plaque morphology and composition in culprit and stable lesions in acute coronary syndrome and stable lesions in stable angina by multidetector computed tomography. J Am Coll Cardiol 2006;47:1655–62.
30. Leber AW, Knez A, Becker A, et al. Accuracy of multidetector spiral computed tomography in identifying and differentiating the composition of coronary atherosclerotic plaques: a comparative study with intracoronary ultrasound. J Am Coll Cardiol 2004;43:1241–7.

31. Schroeder S, Kopp AF, Baumbach A, et al. Noninvasive detection and evaluation of atherosclerotic coronary plaques with multislice computed tomography. J Am Coll Cardiol 2001; 37:1430–5.
32. Matsumoto N, Sato Y, Yoda S, et al. Prognostic value of non-obstructive CT low-dense coronary artery plaques detected by multislice computed tomography. Circ J 2007;71:1898–903.
33. Motoyama S, Sarai M, Harigaya H, et al. Computed tomographic angiography characteristics of atherosclerotic plaques subsequently resulting in acute coronary syndrome. J Am Coll Cardiol 2009;54:49–57.
34. Pundziute G, Schuijf JD, Jukema JW, et al. Prognostic value of multislice computed tomography coronary angiography in patients with known or suspected coronary artery disease. J Am Coll Cardiol 2007;49:62–70.
35. van Werkhoven JM, Schuijf JD, Gaemperli O, et al. Incremental prognostic value of multi-slice computed tomography coronary angiography over coronary artery calcium scoring in patients with suspected coronary artery disease. Eur Heart J 2009;30: 2622–9.
36. Russo V, Zavalloni A, Bacchi Reggiani ML, et al. Incremental prognostic value of coronary CT angiography in patients with suspected coronary artery disease. Circ Cardiovasc Imaging 2010;3:351–9.
37. Becker CR, Nikolaou K, Muders M, et al. Ex vivo coronary atherosclerotic plaque characterization with multi-detector-row CT. Eur Radiol 2003; 13:2094–8.
38. Ferencik M, Chan RC, Achenbach S, et al. Arterial wall imaging: evaluation with 16-section multidetector CT in blood vessel phantoms and ex vivo coronary arteries. Radiology 2006; 240:708–16.
39. Leber AW, Becker A, Knez A, et al. Accuracy of 64-slice computed tomography to classify and quantify plaque volumes in the proximal coronary system: a comparative study using intravascular ultrasound. J Am Coll Cardiol 2006;47:672–7.
40. Cademartiri F, Mollet NR, Runza G, et al. Influence of intracoronary attenuation on coronary plaque measurements using multislice computed tomography: observations in an ex vivo model of coronary computed tomography angiography. Eur Radiol 2005; 15:1426–31.
41. Pohle K, Achenbach S, Macneill B, et al. Characterization of non-calcified coronary atherosclerotic plaque by multi-detector row CT: comparison to IVUS. Atherosclerosis 2007;190: 174–80.
42. Sarwar A, Rieber J, Mooyaart EA, et al. Calcified plaque: measurement of area at thin-section flat-panel CT and 64-section multidetector CT and comparison with histopathologic findings. Radiology 2008;249:301–6.
43. Motoyama S, Kondo T, Sarai M, et al. Multislice computed tomographic characteristics of coronary lesions in acute coronary syndromes. J Am Coll Cardiol 2007;50:319–26.
44. Leber AW, Knez A, White CW, et al. Composition of coronary atherosclerotic plaques in patients with acute myocardial infarction and stable angina pectoris determined by contrast-enhanced multislice computed tomography. Am J Cardiol 2003;91:714–8.
45. Achenbach S, Boehmer K, Pflederer T, et al. Influence of slice thickness and reconstruction kernel on the computed tomographic attenuation of coronary atherosclerotic plaque. J Cardiovasc Comput Tomogr 2010;4: 110–5.

Key Words: computed tomography ■ coronary artery disease ■ histopathology ■ napkin-ring sign ■ plaque attenuation pattern ■ vulnerable coronary plaque.